

This article was downloaded by: [Stanford University Libraries]

On: 04 October 2012, At: 06:36

Publisher: Taylor & Francis

Informa Ltd Registered in England and Wales Registered Number: 1072954

Registered office: Mortimer House, 37-41 Mortimer Street, London W1T 3JH, UK



## Philosophical Magazine A

Publication details, including instructions for authors and subscription information:

<http://www.tandfonline.com/loi/tpha20>

### Estimating grain-size distributions in nanocrystalline materials from X-ray diffraction profile analysis

C. E. Kril<sup>a</sup> & R. Birringer<sup>a</sup>

<sup>a</sup> Universität des Saarlandes, FB 10 Physik, Gebäude 43, Postfach 151150, D-66041, Saarbrücken, Germany

Version of record first published: 12 Aug 2009.

To cite this article: C. E. Kril & R. Birringer (1998): Estimating grain-size distributions in nanocrystalline materials from X-ray diffraction profile analysis, *Philosophical Magazine A*, 77:3, 621-640

To link to this article: <http://dx.doi.org/10.1080/01418619808224072>

PLEASE SCROLL DOWN FOR ARTICLE

Full terms and conditions of use: <http://www.tandfonline.com/page/terms-and-conditions>

This article may be used for research, teaching, and private study purposes. Any substantial or systematic reproduction, redistribution, reselling, loan, sub-licensing, systematic supply, or distribution in any form to anyone is expressly forbidden.

The publisher does not give any warranty express or implied or make any representation that the contents will be complete or accurate or up to date. The accuracy of any instructions, formulae, and drug doses should be independently verified with primary sources. The publisher shall not be liable for any loss, actions, claims, proceedings, demand, or costs or damages whatsoever or howsoever caused arising directly or indirectly in connection with or arising out of the use of this material.

## Estimating grain-size distributions in nanocrystalline materials from X-ray diffraction profile analysis

By C. E. KRILL and R. BIRRINGER

Universität des Saarlandes, FB 10 Physik, Gebäude 43, Postfach 151150,  
D-66041 Saarbrücken, Germany

[Received 3 March 1997 and accepted in revised form 30 June 1997]

### ABSTRACT

It is well known that the Fourier analysis of X-ray diffraction peak profiles (as implemented by Warren and Averbach) can accurately determine the area-weighted average grain size of a fine-grained sample. Less well known is the fact that this method simultaneously yields a volume-weighted average grain size. Under certain circumstances, knowledge of these two weighted average grain sizes is sufficient to permit reliable estimation of the grain-size distribution, even when the distribution cannot be calculated directly from the Fourier coefficients, as is usually the case. We demonstrate this for a nanocrystalline Pd sample prepared by inert-gas condensation; **average grain sizes and the grain-size distribution are estimated by X-ray diffraction profile analysis and compared with the same quantities measured directly by transmission electron microscopy (TEM).** Very good agreement between the resulting average grain sizes is achieved only after compensating for the fact that diffraction profile analysis directly yields an average unit-cell column length rather than an average grain diameter. The agreement between the grain-size distributions determined by profile analysis and TEM was good for crystallite sizes larger than the area-weighted average grain size but deteriorated for smaller sizes due to the volume dependence of the diffraction peak intensity.

### §1. INTRODUCTION

As the name suggests, nanocrystalline materials are made up of crystallites having characteristic sizes between about 2 and 50 nm. The typical crystallite sizes in conventional polycrystalline materials are several orders of magnitude larger. This difference can manifest itself in unusual or enhanced mechanical, magnetic or transport properties in the nanocrystalline state. For such properties, the deviation from conventional behaviour is a sensitive function of the crystallite-size distribution. Therefore, when comparing nanocrystalline materials with conventional materials, one must have a reliable method for measuring the average crystallite size and the crystallite-size distribution.

There are two basic approaches to measuring crystallite sizes in nanocrystalline materials: direct imaging using transmission electron microscopy (TEM) and indirect measurement using X-ray diffraction. Direct imaging is capable of yielding the entire distribution of crystallite sizes in a sample, but it requires time-consuming and often challenging sample preparation and image analysis. Furthermore, the volume that one can examine in the microscope is always very small in comparison with the entire sample, leading to uncertainty as to whether a truly characteristic region of the sample was investigated. X-ray diffraction, on the other hand, averages over a much larger fraction of the sample, and the necessary sample preparation is often

minimal. Unfortunately, the usual methods for analyzing wide-angle X-ray diffraction data generally yield simply an average crystallite size rather than the entire crystallite-size distribution. Even more sophisticated techniques, such as the Fourier analysis of diffraction peak profiles, have limited ability to determine crystallite-size distributions in samples containing a significant amount of inhomogeneous strain.

In this paper we propose a method for estimating the grain-size distribution in a nanocrystalline material from the results of a Fourier analysis of X-ray diffraction peak profiles. This technique is applicable even when mathematical instability prevents calculation of the grain-size distribution by direct differentiation of the Fourier coefficients. Our method presupposes that the mathematical form of the distribution function is known independently, a condition that is often met for nanocrystalline samples, since the distribution form in such materials is frequently determined by the sample preparation technique. The reliability of the grain-size distribution analysis is evaluated by comparing the X-ray diffraction results with those of a TEM study performed on the same sample.

## §2. THEORY

The measurement of grain sizes by means of X-ray diffraction has been a subject of experimental and theoretical interest for nearly 80 years, and the literature on the subject is correspondingly extensive. In this section we summarize many of the concepts and results important to the data analysis that will be performed in subsequent sections; detailed information can be found in the indicated references.

### 2.1. Unit-cell columns

Scherrer demonstrated in 1918 that the size of a diffracting crystallite† is directly related to the width of the X-ray diffraction peaks arising from its crystalline structure (Warren 1990). For crystallite sizes less than about 100 nm, this size-induced peak-broadening effect may be measured accurately enough to deduce an average grain size in the sample. Bertaut (1949, 1950) introduced the concept of considering a crystallite to be composed of "unit-cell columns" aligned perpendicularly to a given set of reflecting planes and extending from one edge of the crystallite to the other. This construction was motivated by his finding that the total diffracted intensity for a given Bragg reflection from a crystallite is simply the sum of the individual intensities diffracted (independently) by each of the unit-cell columns making up the crystallite. Since the individual crystallites contained in a sample also scatter independently, the total diffracted intensity from a collection of crystallites is just the sum of the intensities diffracted by all the unit-cell columns in the irradiated volume.

In other words, it is the distribution of unit-cell column lengths, rather than the distribution of crystallite sizes, that governs the diffraction of X-rays from a polycrystalline sample. The grain-size-induced contribution to the total Bragg-peak broadening must therefore be a function solely of the *column-length distribution*  $p(L)$ , where  $L$  is the length of a unit-cell column. Standard methods for analysing size-induced peak broadening, such as the Scherrer formula (Warren 1990) or the Williamson–Hall (1953) size–strain analysis, provide an estimate solely for the

---

† In this paper the terms *crystallite* and *grain* are used interchangeably to refer to the crystalline units separated by grain boundaries that make up a polycrystalline material.

volume-weighted average column length  $\langle L \rangle_{\text{vol}}$ . A Fourier analysis of the Bragg peak profiles, on the other hand, can in principle deliver complete information regarding  $p(L)$  for  $L \lesssim 100$  nm (Warren 1990); usually, however, such an analysis is capable of providing reliable values for only two weighted average column lengths:  $\langle L \rangle_{\text{area}}$  and  $\langle L \rangle_{\text{vol}}$  (Wagner 1966). The latter quantities are defined and discussed in appendix A.

### 2.2. Converting column lengths to crystallite sizes

If we designate the size of an individual grain by the symbol  $D$ , then the size distribution of a large number of crystallites can be approximated by a continuous function  $g(D)$  (appendix A). For a given sample the *grain-size distribution function*  $g(D)$  generally differs quite significantly from the column-length distribution function  $p(L)$ . Typically, we are interested in measuring the former, but X-ray diffraction (as indicated above) directly measures only the latter. Converting  $p(L)$  to  $g(D)$  requires knowledge of the shape of each crystallite, since the distribution of column lengths in a given grain is related to the grain's geometric boundaries.

For the case when all the crystallites of a sample have roughly the same shape, Smith (1976) has derived the general relation between the two distributions:

$$p(L) = N \int_0^{\infty} f(L, D)g(D) dD, \quad (1)$$

where  $N$  is a normalization factor and  $f(L, D) dL$  is the number of columns normal to the reflecting planes with lengths between  $L_0$  and  $L_0 + dL$  in a single crystallite of size  $D_0$ . Note that  $f(L, D) = 0$  if  $D_0$  is too small to accommodate a column of length  $L_0$  for the assumed shape. For spherical crystallites,

$$f_{\text{sphere}}(L, D) = \begin{cases} \frac{\pi}{2} L & \text{if } L \leq D, \\ 0 & \text{if } L > D, \end{cases} \quad (2)$$

valid for all reflections ( $hkl$ ) (Smith 1976). For all other shapes, it is difficult to derive expressions for  $f(L, D)$  that hold for the general case of orientational averaging (i.e. when the relative orientation between the crystallite boundaries and the crystallite planes is random); nevertheless, Goodisman (1980) has succeeded in developing a method for determining  $f(L, D)$  for orientationally averaged space-filling rectangular prisms and rhombohedrons. In appendix B we make use of his expression of  $f(L, D)$  for cubic crystallites.

### 2.3. Estimating $g(D)$ from diffraction data

As will be seen below, complete information regarding the column-length distribution  $p(L)$  is contained in the Fourier coefficients of the Bragg-peak profiles measured in a diffraction experiment. After correction for instrumental broadening (Klug and Alexander 1974), a Bragg-peak profile may be expressed as a Fourier series having the following form:

$$f(s) \propto \sum_{L=-\infty}^{\infty} \{A(L) \cos [2\pi(s - s_0)L] + B(L) \sin [2\pi(s - s_0)L]\}, \quad (3)$$

where  $L$  is the (real-space) conjugate variable to  $s - s_0$  and  $A(L)$  and  $B(L)$  are the cosine and sine Fourier coefficients respectively. The variable  $s = (2 \sin \theta) / \lambda$  is a function of the diffraction angle  $\theta$  and the X-ray wavelength  $\lambda$ ; the diffraction peak is

assumed to be centred at  $s_0$ . Equations for determining the appropriate set of  $L$  values appearing in eqn. (3) for a given peak are given by Wagner (1966) and Warren (1990). Bertaut (1949, 1950) proved that the quantity  $L$  in eqn. (3) is the length of a column of unit cells perpendicular to the diffracting planes responsible for the Bragg peak (i.e.  $L$  has the same meaning as in §2.1).

Warren and Averbach (1950, 1952) showed that the coefficients  $A(L)$  and  $B(L)$  can be written as the product of a purely size-broadening term and a purely strain-broadening term:  $A(L) = A^{\text{size}}(L)A^{\text{strain}}(L)$ . Furthermore, they developed a procedure for determining the individual size and strain contributions from measurements of two or more orders of the same Bragg reflection (Warren 1959, 1990). This latter step is important for the characterization of most nanocrystalline materials, since the highly non-equilibrium procedures by which they are prepared (e.g. inert-gas condensation + compaction or ball milling) generally lead to the incorporation of significant amounts of inhomogeneous strain.

### 2.3.1. Fourier coefficient differentiation

Bertaut (1949, 1950) proved that it is possible to determine the column-length distribution  $p(L)$  from the second derivative of the cosine Fourier size coefficients  $A^{\text{size}}(L)$ :

$$p(L) = \langle L \rangle_{\text{area}} \frac{d^2 A^{\text{size}}(L)}{dL^2}. \quad (4)$$

From the form of eqn. (1) we see that at least one additional differentiation is necessary to determine  $g(D)$  from  $p(L)$  (Smith 1976). Unfortunately, when the Bragg-peak profiles are corrected for instrumental broadening by deconvolution in Fourier space (Stokes deconvolution (Klug and Alexander 1974)), the  $A^{\text{size}}(L)$  against  $L$  curve is usually superimposed with oscillations arising from the finite cut-off in reciprocal space (Bertaut 1952, Popescu and Benes 1977). Furthermore, counting statistics propagate to cause small shifts in the  $A^{\text{size}}(L)$  values (Wilson 1967, 1968, 1969). Finally, the Warren–Averbach size–strain separation procedure introduces significant additional uncertainties (Delhez *et al.* 1980). These sources of error cause fluctuations in the derivatives of  $A^{\text{size}}(L)$  that grow with increasing number of differentiations. Unless size–strain separation is made superfluous by a lack of inhomogeneous strain in the sample, the noise in  $p(L)$  calculated from  $A^{\text{size}}(L)$  can easily exceed 100%, rendering the values obtained from eqn. (4) meaningless (Delhez *et al.* 1980).

While various techniques have been developed to stabilize the differentiations necessary for calculating  $p(L)$  (Păușescu *et al.* 1974, Le Bail and Louër 1978), such a stabilization process itself can significantly affect the derived distribution function, making it unclear to what extent such methods recover information about the true grain-size distribution function. The additional differentiation required to determine  $g(D)$  from  $p(L)$  further exacerbates the problem.

Two recently developed indirect Fourier analysis methods are able to avoid the oscillations associated with the usual determination of  $A^{\text{size}}(L)$  by direct Fourier transformation. Both the method of Balzar (1992, 1993) and that of Weissmüller *et al.* (1997) show promising results for determining grain-size distributions in samples with moderate levels of internal strain, although extensive comparisons with size distributions measured directly by TEM have yet to be performed.

2.3.2. Known or assumed distribution form

The functional dependence of the cosine Fourier size coefficients  $A^{\text{size}}(L)$  on  $L$  provides two independent weighted average column lengths (Bertaut 1949, 1950, Wagner 1966, Warren 1990);

$$\langle L \rangle_{\text{area}} = -A^{\text{size}}(0) / \lim_{L \rightarrow 0} \left( \frac{dA^{\text{size}}}{dL} \right), \tag{5 a}$$

$$\langle L \rangle_{\text{vol}} = 2 \int_0^\infty A^{\text{size}}(L) dL. \tag{5 b}$$

Using the equations derived in appendix B for converting between weighted average column lengths and grain sizes, one can calculate two independent weighted averages over the grain-size distribution  $g(D)$  (namely  $\langle D \rangle_{\text{area}}$  and  $\langle D \rangle_{\text{vol}}$ ) from the Fourier analysis results. If  $g(D)$  can be approximated by a known function having two free parameters, then these parameters can be determined from  $\langle D \rangle_{\text{area}}$  and  $\langle D \rangle_{\text{vol}}$ .

Estimating  $g(D)$  from two independent moments of the size distribution is not a new idea. Using small-angle X-ray scattering (SAXS), Harkness *et al.* (1969) evaluated two ratios of moments of  $g(D)$  ( $\langle D^3 \rangle / \langle D^2 \rangle$  and  $\langle D^7 \rangle / \langle D^5 \rangle$ ) in samples containing spherical Guinier–Preston (GP) zones. These ratios were then used to determine the parameters of a log-normal approximation for the size distribution of the GP zones. A combination of SAXS and an assumed log-normal distribution form was also employed by Whyte *et al.* (1972) to evaluate particle-size distributions of Pt dispersions on alumina catalysts.†

**That grain-size distributions in nanocrystalline materials made by the inert-gas condensation method can be well described by a log-normal function has been verified experimentally by Granqvist and Buhrman (1976) and Haas and Birringer (1992). The (normalized) log-normal distribution has the form**

$$g_{\text{LN}}(D) = \frac{1}{(2\pi)^{1/2} D \ln \sigma} \exp \left[ -\frac{1}{2} \left( \frac{\ln(D/D_0)}{\ln \sigma} \right)^2 \right], \tag{6}$$

where  $D_0$  and  $\sigma$  are constant parameters describing the median and variance of the distribution respectively and  $\int_0^\infty g_{\text{LN}}(D) dD = 1$ . Substituting eqn. (6) into eqns. (A 3 a) and (A 3 b) yields expressions for the area-weighted average grain size  $\langle D \rangle_{\text{area}}$  and the volume-weighted average grain size  $\langle D \rangle_{\text{vol}}$  in terms of  $D_0$  and  $\sigma$  for a log-normal distribution (Hinds 1982):

$$\langle D \rangle_{\text{area}} = D_0 \exp \left( \frac{2}{3} \ln^2 \sigma \right), \tag{7 a}$$

$$\langle D \rangle_{\text{vol}} = D_0 \exp \left( \frac{7}{2} \ln^2 \sigma \right). \tag{7 b}$$

The quantities  $\langle L \rangle_{\text{area}}$  and  $\langle L \rangle_{\text{vol}}$  can be related to  $D_0$  and  $\sigma$  using eqns. (B 4) and (B 5);

$$\langle L \rangle_{\text{area}} = \frac{2}{3} D_0 \exp \left( \frac{2}{3} \ln^2 \sigma \right) \quad (\text{spheres}), \tag{8 a}$$

$$\langle L \rangle_{\text{vol}} = \frac{3}{4} D_0 \exp \left( \frac{7}{2} \ln^2 \sigma \right) \quad (\text{spheres}), \tag{8 b}$$

---

† Difficulties in accurate data analysis arising from interparticle interference (Weissmüller *et al.* 1995) and pore scattering (Sanders *et al.* 1993) preclude using SAXS to evaluate grain-size distributions in compacted nanocrystalline materials.

assuming spherical grains. If  $\langle L \rangle_{\text{area}}$  and  $\langle L \rangle_{\text{vol}}$  have been measured for a given sample by X-ray diffraction, eqns. (8) can be solved for  $D_0$  and  $\sigma$ , thus fully determining the corresponding log-normal distribution function  $g_{\text{LN}}(D)$ .

Note that this strategy may be followed for any two-parameter distribution function yielding finite  $\langle D \rangle_{\text{area}}$  and  $\langle D \rangle_{\text{vol}}$  values. Furthermore, even when the functional form of  $g(D)$  is not known for a given sample, an estimate for the width of  $g(D)$  can be gained from the ratio of  $\langle D \rangle_{\text{vol}}$  to  $\langle D \rangle_{\text{area}}$ . We now demonstrate the experimental utility of this approach by applying it to a sample of nanocrystalline Pd and comparing the resulting grain-size averages and distribution with those determined by direct observation using TEM.

### §3. EXPERIMENTAL DETAILS

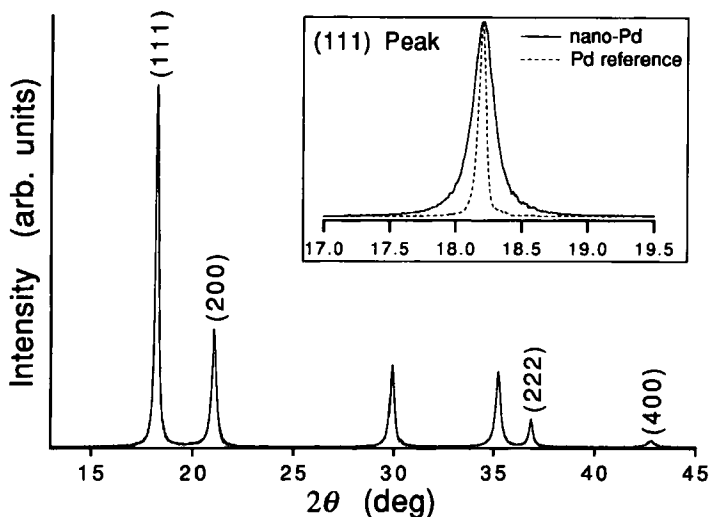
Samples of nanocrystalline Pd were prepared by inert-gas condensation and subsequent compaction (Birringer *et al.* 1984). Pd wire (purity, 99.95%) was evaporated in a W boat into a He (purity, 99.996%) atmosphere of pressure 3 mbar ( $3 \times 10^2$  Pa); the Pd atoms condensed in the gas phase into crystallites, which were then collected by convection onto a liquid-N<sub>2</sub> cooled cold finger. The resulting powder was scraped from the cold finger into a uniaxial press, evacuated to less than  $10^{-6}$  mbar ( $10^{-4}$  Pa), in which the powder was subsequently compacted at room temperature and a pressure of 2 GPa into pellets 8 mm in diameter and 0.2–0.5 mm thick.

All X-ray diffraction measurements were carried out on a Siemens D-5000 diffractometer in  $\theta$ - $\theta$  geometry using Mo K $\alpha$  radiation ( $\lambda = 0.70932 \text{ \AA}$ ). Both the nanocrystalline samples and the reference materials were measured at a step width of  $0.01^\circ$  for typical count times of 20 s. The K $\alpha_2$  component of the scattering was removed using the Rachinger algorithm (Klug and Alexander 1974).

Two different coarse-grained samples were prepared for measuring the instrumental broadening function of the diffractometer: firstly unannealed Pd powder (purity, 99.9+%; particle size less than  $60 \mu\text{m}$ ); secondly unannealed lanthanum hexaboride (LaB<sub>6</sub>) powder (purity, 99%; particle size 5–8  $\mu\text{m}$ ) placed in glass holders. Efforts to increase the grain size of the Pd powder through annealing at temperatures above  $600^\circ\text{C}$  in vacuum resulted in significant sintering of the powder but in no measurable sharpening of the diffraction peaks. LaB<sub>6</sub> powder is known to give extremely sharp diffraction peaks (Balzar 1992, 1993); indeed, the peaks measured from the LaB<sub>6</sub> standard were narrower than those resulting from the Pd standard, implying that a residual amount of size and/or strain broadening was present in the Pd standard. A comparison between analyses made with each reference material was used to judge the significance of the residual Pd broadening on the grain-size analysis (§4.3.1).

TEM was carried out on thin samples of nanocrystalline Pd prepared by embedding pieces of a pellet in epoxy and cutting them with a diamond microtome blade into slices 30–50 nm thick. Dark-field images were recorded at a magnification of  $30\,000\times$  on a JEOL 200CX microscope at 200 kV from the (111) diffraction ring. Subsequent image analysis was performed by digitizing images with a video camera connected to a personal computer. Processing of the digitized images was carried out using standard image analysis software.

Fig. 1



X-ray diffraction scan of an inert-gas-condensed nanocrystalline Pd pellet. The inset compares the (111) peak of nanocrystalline Pd with that of the coarse-grained Pd reference.

#### §4. RESULTS

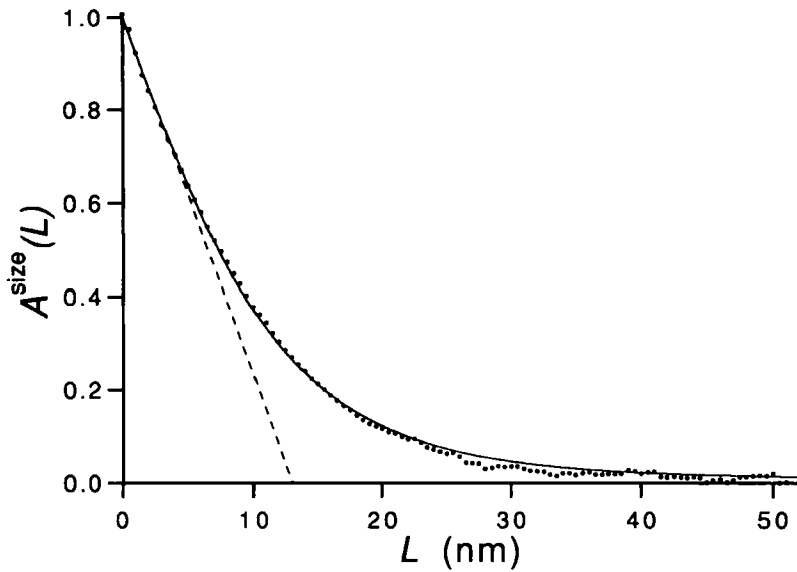
##### 4.1. X-ray diffraction of nanocrystalline Pd

Diffraction scans of a nanocrystalline Pd pellet and of the Pd standard are displayed in fig. 1. The Warren–Averbach Fourier analysis (Warren 1990) was carried out on both the (111)–(222) and the (200)–(400) diffraction peak pairs. This necessitated removal of adjacent peaks by fitting them with a Lorentzian (Cauchy) function, subtracting the fitted curve from the overall scan and smoothing out noise near the former position of the removed peak. Deconvolution of instrumental broadening was carried out by the Stokes method (Klug and Alexander 1974), and the Fourier transformations were calculated using a fast Fourier transform (FFT) routine (Press *et al.* 1989). After deconvolution, each peak profile was corrected for the angular dependence of the Lorentz, polarization and atomic scattering factors (Delhez *et al.* 1980). Values for  $A^{\text{size}}(L)$  and the rms inhomogeneous strain  $\langle \epsilon^2(L) \rangle^{1/2}$  as a function of  $L$  were calculated from the diffraction pairs using a modified version of the strain-correction equation proposed by Warren and Averbach (Delhez *et al.* 1980):

$$A(L) \approx A^{\text{size}}(L) \left( 1 - \frac{2\pi^2}{d^2} \langle \epsilon^2(L) \rangle L^2 \right), \quad (9)$$

where  $d$  is the spacing of the diffracting planes. According to Delhez *et al.* (1980), the Fourier size coefficients  $A^{\text{size}}(L)$  derived from eqn. (9) are less sensitive than those derived from the equation of Warren and Averbach to statistical errors in the measurement of the second-order reflection, which is usually subject to greater uncertainty than the first-order peak owing to the second-order peak's reduced

Fig. 2



Plot of normalized cosine Fourier size coefficients  $A^{\text{size}}(L)$  (.....) against column length  $L$  calculated from the (111) and (222) diffraction peaks of fig. 1 using the Warren–Averbach method. The instrumental broadening was deconvoluted using the scan of coarse-grained Pd. The area-weighted average column length  $\langle L \rangle_{\text{area}}$  is given by the intercept of the broken line with the  $L$  axis; the volume-weighted average column length  $\langle L \rangle_{\text{vol}}$  is twice the area under the  $A^{\text{size}}(L)$  curve. The solid curve represents the cosine Fourier coefficients of a log-normal distribution of spherical grains having the same area and volume-weighted average sizes as those calculated from the experimentally determined cosine Fourier size coefficients (see § 5.1.2).

intensity. Finally, the resulting  $A^{\text{size}}(L)$  coefficients were normalized such that  $A^{\text{size}}(0) = 1$ .†

The normalized  $A^{\text{size}}(L)$  coefficients evaluated from the (111)–(222) diffraction peak pair are plotted as a function of  $L$  in fig. 2. Here, the tangent used to calculate  $\langle L \rangle_{\text{area}}$  is also indicated (eqn. (5a)); the volume-weighted average column length  $\langle L \rangle_{\text{vol}}$  was calculated from the area beneath the  $A^{\text{size}}(L)$  curve according to eqn. (5b). The conversion between average column length and average grain size was accomplished using eqns. (B4) and (B5), assuming spherical grains. The log-normal grain-size distribution having the same area and volume-weighted grain sizes as those measured by the Warren–Averbach method was then determined by solving eqns. (7) for the parameters  $D_0$  and  $\sigma$ . The results of this analysis are collected in table 1.

† The manner in which this normalization should be carried out is a matter of some controversy, since the very-low- $L$  cosine Fourier size coefficients often display a non-physical ‘hook.’ As suggested by Warren (1990), we determine  $A^{\text{size}}(0)$  by fitting a straight line to the  $A^{\text{size}}(L)$  coefficients at  $L$  values just above the ‘hook’ and extrapolating to  $L = 0$  (Delhez *et al.* 1980). Alternatively, Rothman and Cohen (1969) recommend fitting a straight line to a plot of  $\ln[A^{\text{size}}(L)]$  against  $L$  and extrapolating to  $L = 0$ .

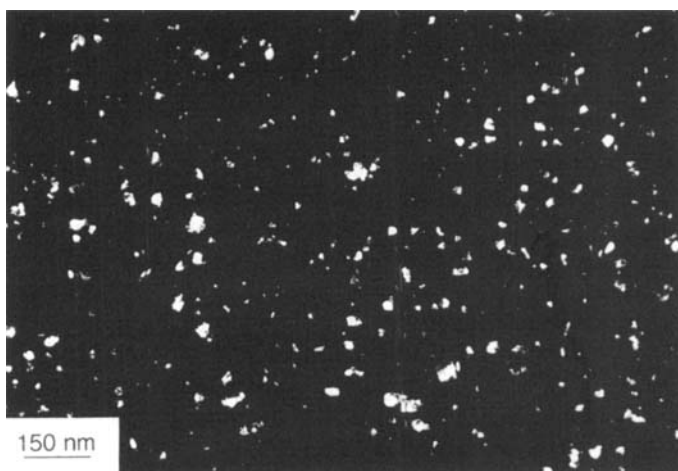
Table 1. Results from the Fourier analysis of the X-ray diffraction scan of inert-gas-condensed Pd (fig. 1). The area-weighted average column lengths  $\langle L \rangle_{\text{area}}$  and volume-weighted average column lengths  $\langle L \rangle_{\text{vol}}$  were calculated from plots of the (111)–(222) and (200)–(400) cosine Fourier size coefficients  $A^{\text{size}}(L)$  against  $L$  as in fig. 2; the scan of coarse-grained Pd was used to deconvolute the instrumental broadening. The remaining columns, namely the area-weighted average grain sizes  $\langle D \rangle_{\text{area}}$ , the volume-weighted average grain sizes  $\langle D \rangle_{\text{vol}}$ , the log-normal distribution parameters  $D_0$  and  $\sigma$ , and the maximum rms strain  $\max [\langle \epsilon^2(L) \rangle^{1/2}]$ , are calculated as described in the text (§4.1). (The rms strain  $\langle \epsilon^2(L) \rangle^{1/2}$  decreases with increasing column length  $L$ . In order to facilitate comparison of strain values,  $\max [\langle \epsilon^2(L) \rangle^{1/2}]$  was determined by extrapolating  $\langle \epsilon^2(L) \rangle^{1/2}$  to  $L = 0$  nm.)

	$\langle L \rangle_{\text{area}}$ (nm)	$\langle L \rangle_{\text{vol}}$ (nm)	$\langle D \rangle_{\text{area}}^{(\text{spheres})}$ (nm)	$\langle D \rangle_{\text{vol}}^{(\text{spheres})}$ (nm)	$D_0$ (nm)	$\sigma$	$\max [\langle \epsilon^2(L) \rangle^{1/2}]$ (%)
(111)–(222)	13.1 ± 1	19.6 ± 1	19.6 ± 1	26.1 ± 1	9.5 ± 3	1.71 ± 0.15	0.31 ± 0.03
(200)–(400)	9.4 ± 1	15.4 ± 1	14.2 ± 1	20.5 ± 1	5.6 ± 2	1.84 ± 0.19	0.47 ± 0.05

#### 4.2. Transmission electron microscopy analysis of nanocrystalline Pd

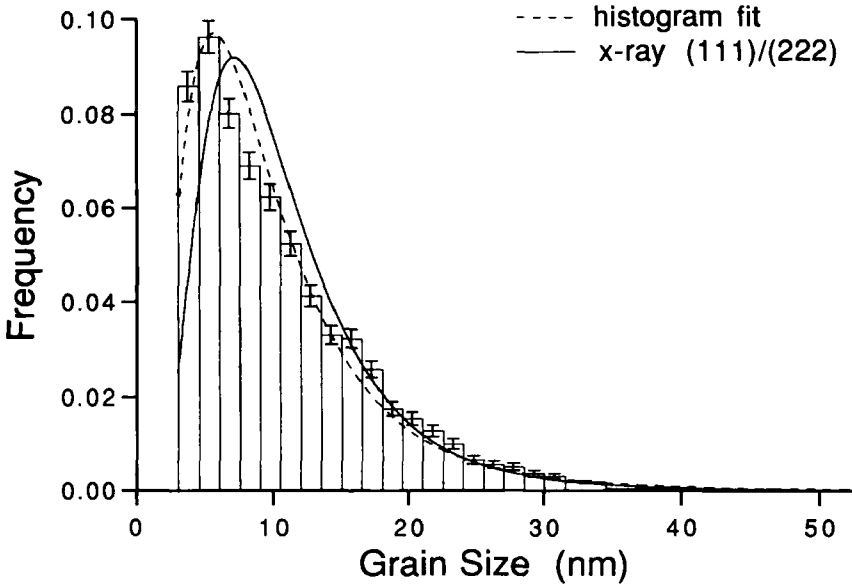
Dark-field images of thin slices from the nanocrystalline Pd sample analysed by X-ray diffraction were obtained by TEM (fig. 3). For the determination of grain sizes, we used the equivalent-circle diameter  $D$ , which is defined in terms of the projected area  $A$  in the image according to  $D = 2(A/\pi)^{1/2}$ ; that is,  $D$  is the diameter of a circle having the area  $A$ . This is a useful measure of grain size in the case of our nanocrystalline samples because the grains are roughly equiaxed, and the thickness of the TEM samples is larger than that of most of the grains. Thus the maximum dimension of the vast majority of grains lies within the sample (rather than partly above or below it because it has been cut off during sample preparation). Since the grains are roughly equiaxed, the maximum dimension of the projected

Fig. 3



Dark-field transmission electron micrograph of inert-gas-condensed Pd. The actual area analysed was approximately 23 times larger than that shown in the figure.

Fig. 4



Histogram of grain sizes in nanocrystalline Pd measured in dark-field TEM micrographs (as in fig. 3) using computer-assisted image analysis. A total of 6150 grains was counted. The broken curve is a weighted least-squares fit of a log-normal distribution function to the count frequencies of the histogram; the fit parameters  $D_0$  and  $\sigma$  are 8.4 nm and 1.88 respectively (table 2). The solid curve is the log-normal distribution determined by Fourier analysis of the (111)–(222) X-ray diffraction peaks assuming spherical grains and using coarse-grained Pd as reference ( $D_0 = 9.5$  nm and  $\sigma = 1.71$ ). The histogram and the log-normal distributions are normalized such that the area under each is unity in the grain-size range covered by the histogram.

grain image will be about the same as the true maximum dimension of each grain. There is therefore no need for stereological correction, and the equivalent-circle diameter as defined above should well approximate the lateral dimension of each grain.

The histogram constructed from image analysis of fig. 3 is displayed in fig. 4. The uncertainties associated with each bin are calculated from the corresponding particle count. Using these uncertainties as weighting factors, we perform a least-squares fit of a log-normal distribution to the histogram (broken line in fig. 4). The good agreement is consistent with the general result that inert-gas-condensed materials display a log-normal size distribution (Granqvist and Buhman 1976, Haas and Birringer 1992). In comparison with the log-normal fit, the histogram appears to be slightly bimodal, a deviation that may have originated during the compaction of the inert-gas-condensed powder into pellet form. Using discrete versions of eqns. (A 2), (A 3 a) and (A 3 b), we calculate  $\langle D \rangle_{\text{num}}$ ,  $\langle D \rangle_{\text{area}}$  and  $\langle D \rangle_{\text{vol}}$  from the list of measured grain sizes (or, equivalently, from the histogram bin frequencies in fig. 4). The results are collected in table 2 together with the parameters  $D_0$  and  $\sigma$  of the log-normal least-squares fit.

Table 2. Comparison of number-, area-, and volume-weighted average grain sizes (assuming spherical crystallite shape) as determined by transmission electron microscopy (TEM) and Fourier analysis (X-ray). The Fourier analysis was carried out using Pd and LaB<sub>6</sub> reference materials to determine instrumental broadening. The log-normal distribution parameters  $D_0$  and  $\sigma$  were determined in the case of TEM analysis from the best-fit log-normal distribution to the histogram in fig. 4, whereas in the Fourier case they were determined from the weighted average grain sizes using eqns. (7). The number-weighted average grain size  $\langle D \rangle_{\text{num}}^{(111)-(222)}$  could be measured directly by TEM but, in the case of X-ray diffraction, had to be calculated from the log-normal distribution parameters using eqn. (10).

	TEM	X-ray	
		Pd reference	LaB <sub>6</sub> reference
$\langle D \rangle_{\text{num}}^{(111)-(222)}$ (nm)	9.8 ± 1	11.0 ± 3	10.1 ± 3
$\langle D \rangle_{\text{area}}^{(111)-(222)}$ (nm)	19.0 ± 2	19.6 ± 1	17.8 ± 1
$\langle D \rangle_{\text{vol}}^{(111)-(222)}$ (nm)	23.2 ± 2	26.1 ± 1	23.5 ± 1
$D_0$ (nm)	8.4 ± 0.1	9.5 ± 3	8.8 ± 3
$\sigma$	1.88 ± 0.02	1.71 ± 0.15	1.70 ± 0.16

### 4.3. Error analysis

#### 4.3.1. X-ray diffraction

Estimating the uncertainty in the grain-size values obtained by X-ray diffraction and TEM image analysis procedures is difficult because, in both cases, systematic uncertainty dominates statistical uncertainty. For the Fourier analysis, uncertainties in the Fourier coefficients arising from counting statistics in the peak profile can be calculated using the formulae derived by Wilson (1967, 1968, 1969); however, for our measurements the resulting statistical uncertainties in  $\langle L \rangle_{\text{area}}$  and  $\langle L \rangle_{\text{vol}}$  were insignificant in comparison with the errors caused by strain correction (eqn. (9)), by Fourier oscillations (arising from the Stokes deconvolution step), by having to place and extrapolate the tangent to the small- $L$  coefficients, and by the non-ideal nature of the reference scan.

As mentioned above (§2.3), the techniques used to prepare materials in a nanocrystalline form generally lead to the incorporation of significant amounts of inhomogeneous strain  $\langle \epsilon^2(L) \rangle^{1/2}$ . The accuracy of the strain correction equation (eqn. (9)) decreases with increasing  $\langle \epsilon^2(L) \rangle L^2$ , where  $L$  is the unit-cell column length. Therefore either large  $\langle \epsilon^2(L) \rangle^{1/2}$  or large  $L$  can lead to errors in the values of  $A^{\text{size}}(L)$  calculated using eqn. (9). Since the quantity  $\langle L \rangle_{\text{area}}$  is determined from the  $A^{\text{size}}(L)$  values at small  $L$  (eqn. (5a)),  $\langle L \rangle_{\text{area}}$  should be insensitive to errors in the strain correction of eqn. (9) (Warren 1990). On the other hand,  $\langle L \rangle_{\text{vol}}$  is calculated by an integration of  $A^{\text{size}}(L)$  over  $L$  (eqn. (5b)); therefore  $\langle L \rangle_{\text{vol}}$  is expected to be highly sensitive to inaccuracies in the strain correction of the cosine Fourier coefficients at large  $L$ . This is mitigated by the fact that the strain correction term in eqn. (9) is proportional to  $A(L)$  itself, which falls rapidly to zero with increasing  $L$ , resulting in small absolute errors in  $A^{\text{size}}(L)$  at large  $L$ . Hence, significant systematic errors in  $\langle L \rangle_{\text{vol}}$ , as calculated from eqn (5b), usually arise only when  $\langle \epsilon^2(L) \rangle^{1/2}$  is large.

Practical experience has shown that the grain-size values determined by X-ray diffraction and TEM fall within about 10% of each other when  $\max\{\langle\epsilon^2(L)\rangle^{1/2}\} \lesssim 0.5\%$ , as was the case for the Pd samples investigated here. Of the nanocrystalline samples we have characterized by X-ray diffraction, the majority of those that were prepared by inert-gas condensation, electrolytic deposition or chemical precipitation meet this condition; ball-milled samples, on the other hand, generally contain significantly higher amounts of inhomogeneous strain (for example Wagner *et al.* (1992)). The applicability of eqn. (9) in the case of ball-milled samples has been called into question by van Berkum *et al.* (1994), who derived an alternative strain correction equation for highly strained materials. The values for  $\langle L \rangle_{\text{area}}$  derived from the alternative analysis differed considerably from those derived from eqn. (9) applied to a diffraction measurement of ball-milled Mo powder. Since no check of the true grain size was performed by TEM, it is not known with certainty that eqn. (9) failed in this case. Nevertheless, it is likely that the method proposed in this paper for estimating the grain-size distribution from  $\langle L \rangle_{\text{area}}$  and  $\langle L \rangle_{\text{vol}}$  values is inapplicable to most ball-milled and other highly strained materials.

For samples containing moderate to little amounts of inhomogeneous strain, the major source of systematic error in the values derived for  $\langle L \rangle_{\text{area}}$  and  $\langle L \rangle_{\text{vol}}$  arises from the correction for instrumental broadening. This requires an 'ideal' reference material with large grains ( $\langle D \rangle_{\text{num}} \gtrsim 1 \mu\text{m}$ ), no strain ( $\langle\epsilon^2(L)\rangle^{1/2} = 0$ ) and the same absorption coefficient as the sample to be measured (Delhez *et al.* 1980, van Berkum *et al.* 1995). These conditions are usually impossible to meet in practice. We have estimated this component of the systematic error by comparing the results obtained using two different non-ideal reference materials: coarse-grained Pd and LaB<sub>6</sub> powder. The latter sample gave sharper peaks than the former, implying that the Pd standard exhibited a certain amount of size and/or strain broadening. A comparison of the grain sizes in table 2 indicates that the values obtained with the LaB<sub>6</sub> standard are about 10% smaller than those obtained with the Pd standard. Since the generation of an 'ideal' reference scan from LaB<sub>6</sub> data is subject to its own uncertainties (van Berkum *et al.* 1995), one cannot be sure that the LaB<sub>6</sub>-calculated sizes are closer to the true average sizes than the Pd sizes, but it seems likely that the Pd-calculated values are somewhat too large. The fact that the TEM-calculated values lie closer to those calculated from the LaB<sub>6</sub> standard lends support to this conclusion. In the literature, uncertainties in average column lengths as calculated by the Warren–Averbach method are generally assumed to be about 5–10% (for example Boldrick *et al.* (1992)); an error of  $\pm 1 \text{ nm}$  (about 5%) covers the spread between our Pd- and LaB<sub>6</sub>-calculated sizes and was therefore assigned to the corresponding  $\langle L \rangle_{\text{area}}$  and  $\langle L \rangle_{\text{vol}}$  values.

#### 4.3.2. Transmission electron microscopy

In the case of image analysis of transmission electron micrographs, the systematic errors again outweigh the statistical uncertainties once a sufficient number of grains has been measured. For the histogram in fig. 4, which was constructed from 6150 grain measurements, the relative statistical uncertainties in  $\langle D \rangle_{\text{num}}$ ,  $\langle D \rangle_{\text{area}}$  and  $\langle D \rangle_{\text{vol}}$  were just 0.88%, 1.3% and 1.9% respectively. Since only a small region of the sample was investigated, and since image analysis introduces its own systematic errors (such as when setting the grey-scale threshold for establishing crystallite boundaries), the total relative systematic uncertainty probably exceeds

5% for grain-size determination. In table 2 we have therefore assigned a relative error of 10% as the total uncertainty in the TEM measurements.

The uncertainties in the log-normal fit parameters  $D_0$  and  $\sigma$  were calculated either from the error matrix of the least-squares fit to the histogram in fig. 4 (see log-normal parameters in the column headed TEM in table 2) or from standard error-propagation formulae for the parameters determined from X-ray data (Bevington 1969). Such formulae were also used to calculate the uncertainty in the  $\langle D \rangle_{\text{num}}^{(111)-(222)}$  values in table 2 calculated from the resulting log-normal distributions (see § 5.1.1).

## § 5. DISCUSSION

### 5.1. Comparison of X-ray diffraction and transmission electron microscopy results

#### 5.1.1. Weighted average grain sizes

Examination of the area-weighted and volume-weighted average grain diameters in table 2 results in good agreement between the  $\langle D \rangle_{\text{area}}$  and  $\langle D \rangle_{\text{vol}}$  values as determined by TEM and X-ray diffraction. Comparing the TEM values in table 2 with the  $\langle L \rangle_{\text{area}}$  and  $\langle L \rangle_{\text{vol}}$  values in table 1 indicates that the agreement between the TEM and X-ray results would have been substantially worse had we not performed the conversion between average column length and average grain size, a frequently neglected correction.

As discussed in § 2.3.2, although the Fourier analysis technique can be used to determine only two weighted average grain sizes directly, knowledge of the form of the grain-size distribution function  $g(D)$  may make it possible to calculate the other average sizes. In the case of inert-gas-condensed Pd,  $g(D)$  is known to be log-normal in form (Haas and Birringer 1992), and the distribution parameters  $D_0$  and  $\sigma$  can be determined from  $\langle D \rangle_{\text{area}}$  and  $\langle D \rangle_{\text{vol}}$  using eqns. (7). From these parameters, for example, the number-weighted average grain size can be calculated (Hinds 1982):

$$\langle D \rangle_{\text{num}} = D_0 \exp\left(\frac{1}{2} \ln^2 \sigma\right). \quad (10)$$

The  $\langle D \rangle_{\text{num}}$  values in table 2 indicate good agreement between the number-weighted average grain size determined by TEM and that calculated from X-ray diffraction, although this may be accidental, since error propagation through eqn. (10) yields a large uncertainty (about 30%) in the  $\langle D \rangle_{\text{num}}$  values calculated from diffraction data.

In order to perform the conversion between average column length and average grain size, one must assume a characteristic geometrical form for the crystallites. In tables 1 and 2 we have assumed spherical grains, but the same calculations could have been carried out just as well assuming another characteristic shape. Using eqns (B6) we can determine the area- and volume-weighted average grain sizes for an assemblage of cube-shaped grains having the  $\langle L \rangle_{\text{area}}$  and  $\langle L \rangle_{\text{vol}}$  values determined by Fourier analysis:  $\langle D \rangle_{\text{area}}^{\text{cubes}} = 24.3 \pm 2$  nm and  $\langle D \rangle_{\text{vol}}^{\text{cubes}} = 27.1 \pm 1$  nm, where column-length averages were determined from (111)–(222) peaks and deconvolution was performed using the Pd reference. These values are in substantially poorer agreement with the TEM-determined values than those calculated under the assumption of spherical grains (table 2). Calculating the log-normal distribution parameters corresponding to these average grain sizes for cube-shaped crystallites, we find that  $D_0 = 18.5 \pm 5.5$  nm and  $\sigma = 1.39 \pm 0.19$ . A mere glance at the histogram in fig. 4

confirms that these values are far less reasonable than those determined under the assumption of spherical grains. Therefore we can conclude that the average crystalline shape in the inert-gas-condensed nanocrystalline Pd sample is more closely spherical than cubic.

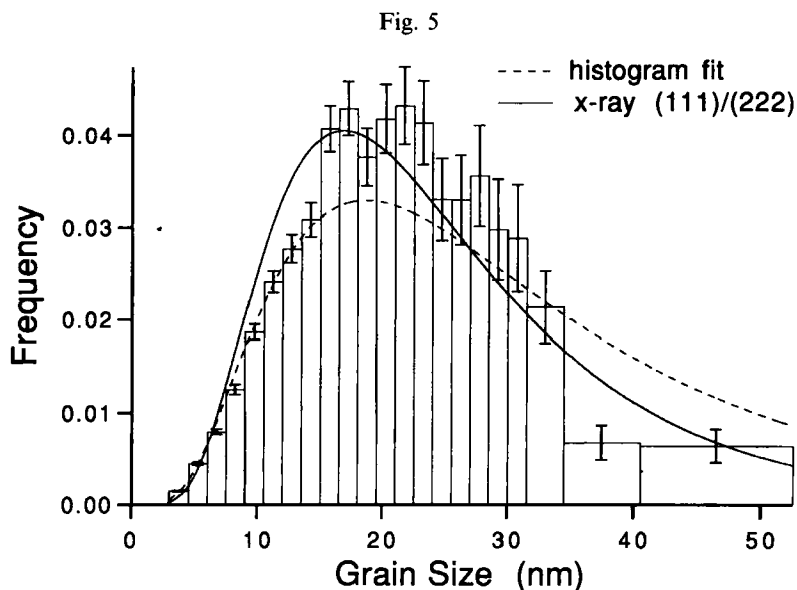
### 5.1.2. Grain-size distributions

As discussed in §2.3.1, direct differentiation of the cosine Fourier size coefficients  $A^{\text{size}}(L)$  to obtain the column-length distribution  $p(L)$  using eqn. (4) is nearly always unsuccessful owing to the magnification of errors that occurs during differentiation; this was confirmed for the data in fig. 2. We can, however, use the reverse process, namely integration of eqn. (4), to evaluate the goodness of fit of the log-normal size distribution calculated from the experimentally determined  $\langle D \rangle_{\text{area}}$  and  $\langle D \rangle_{\text{vol}}$  values. Using the log-normal distribution parameters in table 1, we employ eqns. (1), (2) and (6) to calculate  $p(L)$ . We then solve eqn. (4) for the  $A^{\text{size}}(L)$  values corresponding to this column-length distribution and plot the resulting coefficients as the solid curve in fig. 2. The agreement between the measured and calculated coefficients is surprisingly good throughout the measurable column-length range, lending support to our contention that the grain-size distribution is well described by a log-normal function.

Despite this close fit, the log-normal distribution function determined by X-ray diffraction differs somewhat from that determined by a fit to the histogram of grain sizes resulting from image analysis (solid and broken curves respectively in fig. 4). Deviations are most apparent at the smallest grain sizes while, above about 15 nm, the curves fall within the uncertainty bounds of the individual histogram bins. This behaviour is not surprising, since the X-ray log-normal distribution was determined solely from the values for  $\langle D \rangle_{\text{area}}$  and  $\langle D \rangle_{\text{vol}}$ , both of which lie at larger grain sizes. The integrated intensity of the X-ray diffraction signal from a single crystallite is proportional to the grain volume; hence the accuracy of grain-size information gained from X-ray diffraction should be highest near the volume-weighted average grain size. This is evident in a comparison of the volume-weighted size distributions measured by TEM image analysis with those derived from X-ray diffraction (fig. 5). The fit to the volume-weighted frequency histogram is quite good for the curve determined from the (111)–(222) Fourier analysis of diffraction data (solid curve), especially above about 15 nm; here the agreement is noticeably better than that of the volume-weighted log-normal function fitted to the histogram itself (broken curve).

### 5.2. Correcting for stacking faults and twin boundaries

In the previous sections we have assumed that the crystallites making up a nanocrystalline sample contain no defects, that is that each grain is a tiny single crystal. Most crystalline materials, however, contain a variety of defects, such as vacancies, pores, dislocations, stacking faults and twin boundaries. The latter two are known to reduce the apparent grain size calculated from diffraction peak broadening (Wagner 1966, Warren 1990). Such defects decrease the spatial extent of the columns contributing to the coherent scattering of X-rays; that is, the size of the resulting 'coherent scattering region' (CSR) bounded by the defects (and grain boundaries) is smaller than that of the crystallite containing the defect(s). Only if the crystallites in a sample contain no stacking faults or twin boundaries are the average sizes  $\langle D \rangle_{\text{area}}$  and  $\langle D \rangle_{\text{vol}}$  (calculated from  $\langle L \rangle_{\text{area}}$  and  $\langle L \rangle_{\text{vol}}$  respectively) estimates for the true area- and volume-weighted average grain sizes. Since stacking



Volume-weighted grain-size distributions for nanocrystalline Pd calculated from the histogram and curves in fig. 4. The (volume-weighted) histogram and the volume-weighted log-normal distributions are normalized such that the area under each is unity in the grain-size range covered by the histogram.

faults or twins are nearly always present to some extent in real materials, the  $\langle D \rangle_{\text{area}}$  and  $\langle D \rangle_{\text{vol}}$  values calculated from diffraction analysis are actually area- and volume-weighted average CSR sizes rather than the desired weighted average grain sizes.

This problem is not limited to X-ray diffraction, however. The same defects that reduce the apparent grain size in diffraction measurements can also limit the spatial extent of crystallites imaged by dark-field techniques in TEM. The effect of twin boundaries on the CSRs seen in dark-field TEM is identical with that measured by X-ray diffraction. Stacking faults, on the other hand, are handled differently by these techniques: coherent scattering generally ends at a stacking fault in both X-ray diffraction and TEM, but the diffraction conditions employed in ordinary dark-field microscopy lead to simultaneous imaging of the CSRs on both sides of the stacking fault, rendering the stacking fault invisible. The size distributions of CSRs seen by X-ray diffraction and by dark-field TEM differ therefore according to the number density of stacking faults.

For materials having fcc symmetry, such as our Pd samples, it is possible to determine the stacking-fault probability  $\alpha$  from peak-shift measurements (Wagner 1966, Warren 1990). The most accurate way to determine peak shifts is to measure the intervals between adjacent peak pairs, such as (111)–(200) or (222)–(400), in a nanocrystalline sample and to compare them with the corresponding intervals in a coarse-grained reference made of the same material. Using the equations given by Warren (1990) relating peak shifts to  $\alpha$ , we find that  $\alpha \approx 0$  for our nanocrystalline Pd sample, within the uncertainty of the measurements. Hence, the CSR size distributions observed by X-ray diffraction and dark-field TEM should be identical in our sample.

The presence of stacking faults or twin boundaries in a nanocrystalline material leads to a dependence of  $\langle L \rangle_{\text{area}}$  and  $\langle L \rangle_{\text{vol}}$  on the Bragg-peak pair used in the Fourier analysis (Wagner 1966, Warren 1990). According to Warren (1990), the difference between  $\langle L \rangle_{\text{area}}^{(111)-(222)}$  and  $\langle L \rangle_{\text{area}}^{(200)-(400)}$  is directly related to a weighted overall faulting probability  $1.5\alpha + \beta$ , where  $\beta$  is the twinning probability. From this relationship† and the data in table 1, we calculate  $1.5\alpha + \beta \approx \beta = 0.020 \pm 0.007$  for our nanocrystalline Pd sample. This value for  $\beta$  corresponds to the presence, on average, of a twin boundary every  $1/\beta = 50 \pm 17$  (111) planes in the grains of nanocrystalline Pd. Since the separation between (111) planes in Pd is 0.225 nm, the average distance between twins is about  $11 \pm 4$  nm; therefore a significant fraction of the larger grains contain twin boundaries. In fact, from Warren's (1990) treatment of faulting, one can estimate that, in the absence of such twins,  $\langle L \rangle_{\text{area}}$  would be approximately  $18.4 \pm 5$  nm. That is, the area-weighted CSR sizes measured by X-ray diffraction and TEM in our nanocrystalline Pd sample are nearly 30% smaller than the true  $\langle D \rangle_{\text{area}}$ .

### §6. CONCLUSIONS

Comparison of average grain sizes in nanocrystalline Pd measured by TEM and X-ray diffraction indicates that reliable values for the area- and volume-weighted average effective grain sizes (i.e. coherent scattering regions) can be determined by the Fourier analysis of diffraction peak profiles using the method of Warren and Averbach. Since analysis of diffraction data directly yields average column lengths, it is necessary to perform a conversion to average grain size before comparing the resulting values with those determined by microscopy; this conversion was best performed by assuming a spherical average grain shape. A method is developed for estimating the overall grain-size distribution from X-ray diffraction data, provided that the functional form of the distribution is known independently. This idea was tested on inert-gas-condensed Pd, for which the grain-size distribution is expected to be log-normal in shape. At smaller grain sizes the size distribution calculated from diffraction data deviated somewhat from the frequency histogram measured by microscopy but, when the calculated and measured distributions were weighted by the grain volume, the agreement was surprisingly good throughout the range of measured grain sizes. An analysis of the twin-boundary probability in this nanocrystalline Pd sample suggests that the area-weighted average grain sizes measured by X-ray diffraction and TEM are about 30% smaller than the area-weighted average grain size corrected for the presence of faulting.

### ACKNOWLEDGEMENTS

We are grateful to C. N. J. Wagner for introducing us to the Warren–Averbach analysis of X-ray diffraction peak profiles, and we thank J. Weissmüller, H. Gleiter, P. G. Sanders and H. Natter for useful and encouraging conversations. The assistance of G. McMahon (electron microscopy), J. Löffler (X-ray diffraction) and V. Haas (image analysis) was most helpful. This research was funded by the Deutsche Forschungsgemeinschaft (G. W. Leibniz program and SFB 277) and the NATO Postdoctoral Fellowship program (C.E.K.).

† There is a misprint in Warren's equation for  $-(dA_L^S/dL)_{111}$  (Warren 1990, p. 293): the 2 in the denominator should be a 4.

## APPENDIX A

## WEIGHTED AVERAGE GRAIN SIZES AND UNIT-CELL COLUMN LENGTHS

Assuming  $D$  to be a measure for the size of an individual crystallite (Matyi *et al.* 1987), we may define a continuous function  $g(D)$  that approximates the distribution of  $D$  values in a given sample; the number of crystallites having a size between  $D_0$  and  $D_0 + dD$  is defined to be  $g(D_0) dD$  (within a normalization factor). The  $j$ th moment  $\langle D^j \rangle$  of the distribution is defined by

$$\langle D^j \rangle \equiv \left( \int_0^\infty D^j g(D) dD \right) / \left( \int_0^\infty g(D) dD \right), \quad (\text{A } 1)$$

whereby  $g(D)$  is often normalized so that  $\int_0^\infty g(D) dD = 1$ . A variety of characteristic *average grain sizes* may be expressed in terms of the moments of the distribution. For example, the arithmetic mean size  $\langle D \rangle_{\text{num}}$  (also called the number-weighted average size) is defined as

$$\begin{aligned} \langle D \rangle_{\text{num}} &\equiv \left( \int_0^\infty D g(D) dD \right) / \left( \int_0^\infty g(D) dD \right) \\ &= \langle D^1 \rangle. \end{aligned} \quad (\text{A } 2)$$

The arithmetic mean size is by no means the only useful average over the distribution function  $g(D)$ ; depending on the application and/or measurement technique, one often needs a weighted average of  $g(D)$  (Hillard *et al.* 1968, Hinds 1982, Krill and Birringer 1996). The *area-weighted average grain size*  $\langle D \rangle_{\text{area}}$  is computed by weighting  $g(D)$  by the quantity  $kD^2$  proportional to the cross-sectional area of a grain of size  $D$ , where  $k$  is a geometry-specific constant. Similarly, volume weighting is achieved by multiplying  $g(D)$  by a factor  $kD^3$ . Mathematically, the area-weighted and volume-weighted average grain sizes are defined in analogy to  $\langle D \rangle_{\text{num}}$ :

$$\begin{aligned} \langle D \rangle_{\text{area}} &\equiv \left( \int_0^\infty D [kD^2 g(D)] dD \right) / \left( \int_0^\infty kD^2 g(D) dD \right) \\ &= \frac{\langle D^3 \rangle}{\langle D^2 \rangle} \end{aligned} \quad (\text{A } 3 a)$$

$$\begin{aligned} \langle D \rangle_{\text{vol}} &\equiv \left( \int_0^\infty D [kD^3 g(D)] dD \right) / \left( \int_0^\infty kD^3 g(D) dD \right) \\ &= \frac{\langle D^4 \rangle}{\langle D^3 \rangle}. \end{aligned} \quad (\text{A } 3 b)$$

The column-length distribution  $p(L)$  is defined such that  $p(L_0) dL$  is the number of columns having lengths between  $L_0$  and  $L_0 + dL$  (within a normalization constant). The  $j$ th moment of  $p(L)$  is defined exactly as in eqn. (A 1):

$$\langle L^j \rangle \equiv \left( \int_0^\infty L^j p(L) dL \right) / \left( \int_0^\infty p(L) dL \right). \quad (\text{A } 4)$$

Since each unit-cell column is oriented perpendicularly to the atomic planes responsible for a given Bragg diffraction peak, the areas  $\delta a$  of each column projected onto

the diffracting planes (i.e. the column cross-sectional area) are identical. In analogy to eqn. (A 3 a), the area-weighted average column length  $\langle L \rangle_{\text{area}}$  is given by

$$\begin{aligned} \langle L \rangle_{\text{area}} &\equiv \left( \int_0^\infty L [\delta a p(L)] dL \right) / \left( \int_0^\infty \delta a p(L) dL \right) \\ &= \langle L^1 \rangle. \end{aligned} \quad (\text{A } 5)$$

Similarly, the volume of a column of length  $L$  is  $\delta a L$ . The volume-weighted average column length  $\langle L \rangle_{\text{vol}}$  is defined in analogy to eqn. (A 3 b):

$$\begin{aligned} \langle L \rangle_{\text{vol}} &\equiv \left( \int_0^\infty L [\delta a L p(L)] dL \right) / \left( \int_0^\infty \delta a L p(L) dL \right) \\ &= \frac{\langle L^2 \rangle}{\langle L^1 \rangle}. \end{aligned} \quad (\text{A } 6)$$

Note that, because each column has the same cross-sectional area,  $\langle L \rangle_{\text{area}}$  is identical to  $\langle L \rangle_{\text{num}}$ ; therefore the designations 'number-weighted' and 'area-weighted' are interchangeable for the case of column averages. Similarly, the volume-weighted average column length is identical with the length-weighted average column length.

## APPENDIX B

### DERIVING CONVERSION FORMULAE BETWEEN WEIGHTED AVERAGES OF GRAIN-SIZE AND COLUMN-LENGTH DISTRIBUTIONS

If all the grains in a given sample have approximately the same shape, one can derive relationships between the weighted average grain size and column lengths. Here, we calculate conversion formulae for collections of spherical or cubic crystallites.

For the case of spherical grains, replacing  $p(L)$  in eqn. (A 4) by the integral in eqn. (1), substituting the expression for  $f_{\text{sphere}}(L, D)$  from eqn. (2) and reversing the order of integration yields

$$\begin{aligned} \langle L^j \rangle &= \left( \frac{\pi}{2} \int_0^\infty L^{j+1} \int_L^\infty g(D) dD dL \right) / \left( \frac{\pi}{2} \int_0^\infty L \int_L^\infty g(D) dD dL \right) \\ &= \left( \int_0^\infty g(D) \int_0^D L^{j+1} dL dD \right) / \left( \int_0^\infty g(D) \int_0^D L dL dD \right) \\ &= \frac{2}{j+2} \left( \int_0^\infty g(D) D^{j+2} dD \right) / \left( \int_0^\infty g(D) D^2 dD \right) \quad (\text{spheres}). \end{aligned} \quad (\text{B } 1)$$

Using eqn. (A 1), we may express  $\langle L^j \rangle$  in terms of the  $(j+2)$ th and second moments of  $g(D)$ :

$$\langle L^j \rangle = \frac{2}{j+2} \frac{\langle D^{j+2} \rangle}{\langle D^2 \rangle} \quad (\text{spheres}). \quad (\text{B } 2)$$

Calculation of the area- and volume-weighted averages of  $p(L)$  for a collection of spherical crystallites in terms of the area- and volume-weighted averages of  $g(D)$  is now straightforward. Combining eqns. (A 5) and (B 2), we express  $\langle L \rangle_{\text{area}}$  in terms of moments of  $g(D)$ :

$$\langle L \rangle_{\text{area}} = \frac{2}{3} \frac{\langle D^3 \rangle}{\langle D^2 \rangle} \quad (\text{spheres}), \quad (\text{B } 3)$$

which, in conjunction with eqn. (A 3 a), yields the conversion relation between  $\langle L \rangle_{\text{area}}$  and  $\langle D \rangle_{\text{area}}$  for spheres:

$$\langle L \rangle_{\text{area}} = \frac{2}{3} \langle D \rangle_{\text{area}} \quad (\text{spheres}). \quad (\text{B } 4)$$

Similar argumentation for the case of  $\langle L \rangle_{\text{vol}}$  gives

$$\langle L \rangle_{\text{vol}} = \frac{\frac{2}{4} (\langle D^4 \rangle / \langle D^2 \rangle)}{\frac{2}{3} (\langle D^3 \rangle / \langle D^2 \rangle)} = \frac{3}{4} \langle D \rangle_{\text{vol}} \quad (\text{spheres}). \quad (\text{B } 5)$$

For the case of cubic crystallites, we use Goodisman's (1980) expression for the orientationally averaged column-length distribution of a cube  $f_{\text{cube}}(L, D)$ . The complexity of  $f_{\text{cube}}(L, D)$  necessitates numerical evaluation of the integral with respect to  $L$  resulting from the substitution of eqn. (1) into eqn (A 4). In terms of the equivalent-sphere measure  $D = (6/\pi)^{1/3} a$  for a cube of side length  $a$ , our calculations yield the following conversion formulae for orientationally averaged cubic grains (Underwood 1970, Weissmüller *et al.* 1997):

$$\langle L \rangle_{\text{area}} = \frac{2}{3} \left( \frac{\pi}{6} \right)^{1/3} \langle D \rangle_{\text{area}} \approx 0.5373 \langle D \rangle_{\text{area}} \quad (\text{cubes}), \quad (\text{B } 6 a)$$

$$\langle L \rangle_{\text{vol}} \approx 0.7227 \langle D \rangle_{\text{vol}} \quad (\text{cubes}). \quad (\text{B } 6 b)$$

#### REFERENCES

- BALZAR, D., 1992, *J. appl. Crystallogr.*, **25**, 559; 1993, *J. Res. natn. Inst. Stand. Technol.*, **98**, 321.
- BERTAUT, E. F., 1950, *Acta Crystallogr.*, **3**, 14; 1952, *ibid.* **5**, 117.
- BERTAUT, F., 1949, *C. r. hebd. Séanc. Acad. Sci., Paris*, **228**, 187, 492.
- BEVINGTON, P. R., 1969, *Data Reduction and Error Analysis for the Physical Sciences* (New York: McGraw-Hill), chap. 4.
- BIRINGER, R., GLEITER, H., KLEIN, H.-P., and MARQUARDT, P., 1984, *Phys. Lett. A*, **102**, 365.
- BOLDRICK, M. S., YANG, E., and WAGNER, C. N. J., 1992, *J. non-crystalline Solids*, **150**, 478.
- DELHEZ, R., DE KEIJSER, TH. H., and MITTEMEIJER, E. J., 1980, *Accuracy in Powder Diffraction*, National Bureau of Standards Special Publication No. 567, edited by S. Block, and C. R. Hubbard, (Washington, DC: National Bureau of Standards), pp. 213–253.
- GOODISMAN, J., 1980, *J. appl. Crystallogr.*, **13**, 132.
- GRANQVIST, C. G., and BUHRMAN, R. A., 1976, *J. appl. Phys.*, **47**, 2200.
- HAAS, V., and BIRINGER, R., 1992, *NanoStruct. Mater.*, **1**, 491.
- HARKNESS, S. D., GOULD, R. W., and HREN, J. J., 1969, *Phil. Mag.*, **19**, 115.
- HILLARD, J. E., COHEN, J. B., and PAULSON, W. M., 1968, *Ultrafine Grain Ceramics*, Proceedings of the 15th Sagamore Army Materials Research Conference (Syracuse, NY: Syracuse University Press), pp. 73–98.
- HINDS, W. C., 1982, *Aerosol Technology: Properties, Behavior, and Measurement of Airborne Particles* (New York: Wiley), chap. 4.
- KLUG, H. P., and ALEXANDER, L. E., 1974, *X-ray Diffraction Procedures for Polycrystalline and Amorphous Materials*, second edition (New York: Wiley), chap. 9.
- KRILL, C. E., and BIRINGER, R., 1996, *Mater. Sci. Forum*, **225–227**, 263.
- LE BAIL, A., and LOUËR, D., 1978, *J. appl. Crystallogr.*, **11**, 50.
- MATYI, R. J., SCHWARTZ, L. H., and BUTT, J. B., 1987, *Catal. Rev.—Sci. Eng.*, **29**, 41.
- PĂUȘESCU, P., MĂNĂILĂ, R., POPESCU, M., and JIHOVICI, E., 1974, *J. appl. Crystallogr.*, **7**, 281.
- POPESCU, FL., and BENES, L., 1977, *Acta Crystallogr. A*, **33**, 323.
- PRESS, W. H., FLANNERY, B. P., TEUKOLSKY, S. A., and VETTERLING, W. T., 1989, *Numerical Recipes in Pascal: The Art of Scientific Computing* (New York: Cambridge University Press), chap. 12.
- ROTHMAN, R. L., and COHEN, J. B., 1969, *Adv. X-ray Anal.*, **12**, 208.

- SANDERS, P. G., WEERTMAN, J. R., BARKER, J. G., and SIEGEL, R. W., 1993, *Scripta metall. mater.*, **29**, 91.
- SMITH, W. L., 1976, *J. appl. Crystallogr.*, **9**, 187.
- UNDERWOOD, E. E., 1970, *Quantitative Stereology* (London: Addison-Wesley), p. 93.
- VAN BERKUM, J. G. M., SPRONG, G. J. M., DE KEIJSER, TH. H., DELHEZ, R., and SONNEVELD, E. J., 1995, *Powder Diffr.*, **10**, 129.
- VAN BERKUM, J. G. M., VERMEULEN, A. C., DELHEZ, R., DE KEIJSER, T. H., and MITTEMEIJER, E. J., 1994, *J. appl. Crystallogr.*, **27**, 345.
- WAGNER, C. N. J., 1966, *Local Atomic Arrangements studied by X-ray Diffraction*, edited by J. B. Cohen and J. E. Hilliard (New York: Gordon and Breach), pp. 219–269.
- WAGNER, C. N. J., YANG, E., and BOLDRICK, M. S., 1992, *Adv. X-ray Anal.*, **35**, 585.
- WARREN, B. E., 1959, *Progress in Metal Physics*, edited by B. Chalmers and R. King, (Oxford: Pergamon), pp. 147–202; 1990, *X-ray Diffraction* (New York: Dover Publications), chap. 13.
- WARREN, B. E., and AVERBACH, B. L., 1950, *J. appl. Phys.*, **21**, 595; 1952, *ibid.*, **23**, 497.
- WEISSMÜLLER, J., LÖFFLER, J., and KLEBER, M., 1995, *NanoStruct. Mater.*, **6**, 105.
- WEISSMÜLLER, J., LÖFFLER, J., KRILL, C. E., BIRNINGER, R., and GLEITER, H., 1997 (in preparation).
- WHYTE, JR., T. E., KIRKLIN, P. W., GOULD, R. W., and HEINEMANN, H., 1972, *J. Catal.*, **25**, 407.
- WILLIAMSON, G. K., and HALL, W. H., 1953, *Acta metall.*, **1**, 22.
- WILSON, A. J. C., 1967, *Acta Crystallogr.*, **23**, 888; 1968, *Acta Crystallogr. A*, **24**, 478(E); 1969, *ibid.*, **25**, 584.